



Synthesis, characterization and application of wheat bran/zinc aluminium and tea leaves waste/zinc aluminium biocomposites: kinetics and thermodynamics modeling

Yusra Safa^{a,*}, Haq Nawaz Bhatti^b, Misbah Sultan^c, Sana Sadaf^d

^aDepartment of Chemistry, Lahore College for Women University, Lahore, Pakistan, email: yusra_safa@yahoo.com

^bEnvironmental Chemistry Laboratory, Department of Chemistry and Biochemistry, University of Agriculture, Faisalabad, Pakistan, email: hnbhatti2005@yahoo.com

^cInstitute of Chemistry, University of the Punjab, Lahore, Pakistan, email: misbahsultan@ymail.com

^dPunjab Bioenergy Institute, University of Agriculture, Faisalabad, Pakistan, email: sanasadaf@gmail.com

Received 7 November 2015; Accepted 11 February 2016

ABSTRACT

In the current study, synthesis and application of wheat bran/zinc aluminum biocomposite and tea leaves waste/zinc aluminum biocomposite for the elimination of hazardous dyes (Reactive Yellow-41 and Direct Blue-7, respectively) were examined. Diverse parameters were used for the data. Optimum pH for maximum removal of dyes was 4. Dye removal was maximum with increase in biocomposite dose, dye concentration, and temperature. The optimum contact time was detected to be 90 min for Reactive Yellow-41 onto wheat bran/zinc aluminum biocomposite and 120 min for Direct Blue-7 onto tea leaves waste/zinc aluminum biocomposite. The research data were best fitted to Langmuir isotherm and pseudo-second-order kinetic model. Surface sorption of dyes was observed through FT-IR analysis. The changes in surface morphology of both the biocomposites were investigated through SEM. XRD analysis was used to examine the crystallinity of biocomposite. It was inferred that wheat bran/zinc aluminum biocomposite and tea leaves waste/zinc aluminum biocomposite are excellent biosorbents for the removal of dyes from aqueous solutions.

Keywords: Adsorption; Wheat bran/zinc aluminum biocomposite; Tea leaves waste/zinc aluminum biocomposite; Modeling

1. Introduction

Pollution control is one of the principal concerns nowadays. Unprocessed or partially processed wastewaters and industrial waste is discharged into natural environments. Among industrial effluents, dye wastewater from textile and dyestuff industries, is one of the most problematic liquids to treat. Textile, paper,

and plastic industries use bulk of chemicals and dyes for coloring and at the end discharge into water stream [1]. The discharge of dye into wastewaters causes severe environmental hazards; this is because dyes usually have a synthetic and complex aromatic molecular structure, which makes them more stable and difficult to biodegrade [2]. Dyes affect the penetration of light through water and hinder photosynthesis, so causing the natural imbalance [3]. The

*Corresponding author.

dye-polluted water causes mutation, skin ulcer, heart diseases, cancer, and jaundice [4].

Physical and chemical processes are mostly used to treat dye wastewater. These consist of coagulation, flocculation, ozonation, oxidation, ion exchange, and adsorption. But these methods have certain limitations such as not cost-effective, formation of dangerous by-products and high-energy requirements [5].

Biosorption is the removal of contaminants from aqueous solutions by using natural materials. It is a favorable biotechnological method for the elimination of pollutants because it is environmental friendly, economical, quick, and easy to operate [6]. Different agricultural wastes such as sawdust [7], activated carbon [8], orange peel [9], and rice husk [3] have been used for dye elimination purpose. But these are not highly efficient. So, searching for effective and efficient biosorbent is the need of the day [10].

In the present research work, synthesis and application of wheat bran/zinc aluminum biocomposite and tea leaves waste/zinc aluminum biocomposite are done. Different process parameters like pH, dye concentration, contact time, pore size of biocomposite, temperature, and dose of biosorbent are studied. Equilibrium and kinetic modeling are also applied to experimental data. Characterization of biocomposites is done by FT-IR, SEM, and XRD analysis.

2. Materials and methods

2.1. Chemicals

All the relevant chemicals were obtained from Sigma–Aldrich Chemical Co. (USA).

2.2. Synthesis of biocomposite

Wheat bran and tea leaves waste were obtained from the local market. After washing with distilled water, the biomasses were kept in sunlight for 3 d and dried in oven at 60°C for 24 h. After grinding and sieving, the biomass was preserved. For the preparation of biocomposite, small particle size biomass is selected and processed further. Wheat bran/zinc aluminum biocomposite and tea leaves waste/zinc aluminum biocomposite were prepared according to the following method: Zinc nitrate (5 g) and aluminum nitrate (2 g) were dissolved in 100 ml of distilled water with vigorous stirring at 85°C for 30 min. Then 20 ml of 30% NH₃ solution was added gradually to the solution. The mixture was stirred at 85°C for 2 h. The synthesized biocomposites were washed several times with distilled water and dried under vacuum [5].

2.3. Preparation of dyes' solution

In this work, Reactive Yellow-41 and Direct Blue-7 dyes were used. After the formation of stock solution, solutions of different concentrations were formed by diluting the stock solution.

General characteristics of dyes are presented in Table 1.

2.4. Batch biosorption experimental studies

Effect of various parameters such as pH, biocomposite dose, particle size, initial dye concentration, contact time, and temperature on the biosorption of dyes was determined. The amount of absorbed dye was calculated through the following equation:

$$q = (C_o - C_e)V/W \quad (1)$$

where q is the dye sorbed capacity on the biocomposite (mg/g), C_o and C_e are the initial and equilibrium dye concentrations, respectively. V is the dye solution volume (ml) and M is the amount of biocomposite (g). The % sorption was determined as follows:

$$\% \text{ Sorption} = C_o - C_e/C_o \times 100 \quad (2)$$

2.5. Adsorption isotherm studies

Adsorption isotherms are used to determine the biosorption. Langmuir [11] and Freundlich [12] isotherm models are applied on the biosorption data.

2.6. Adsorption kinetics studies

The performance of dyes onto the wheat bran/zinc aluminum biocomposite and tea leaf waste/zinc aluminum biocomposite was examined using the pseudo-first-order [13] and pseudo-second-order [14] kinetic models.

2.7. Desorption/regeneration of biocomposite

All the used biocomposites were treated with distilled water at higher pH. After completion of the

Table 1
General characteristics of dyes

Dye	Color	Type	λ_{max} (nm)
Reactive Yellow-41	Yellow	Reactive	410
Direct Blue-7	Blue	Direct	400

sorption experiment the biocomposite was filtered, dried, and treated with distilled water at pH 10–14. And this biocomposite was again treated with dye solution and the process of adsorption and desorption was repeated five times to check the desorption capacity of the biocomposite.

% Desorption is calculated as:

$$\% \text{ Desorption} = \frac{\text{Amount of desorbed dye} \left(\frac{\text{mg}}{\text{g}} \right)}{\text{Amount of adsorbed dye} \left(\frac{\text{mg}}{\text{g}} \right)} \times 100 \quad (3)$$

3. Results and discussion

3.1. Effect of pH

The pH of the solution greatly affects the dye removal capacity. Dye molecule ionization and sorption processes are affected by a change in the pH of the medium. Removal of dyes is influenced by changing the pH of the solution [15]. To determine the optimum pH of Reactive Yellow-41 and Direct Blue-7 dyes, experiments were done from 2 to 8 pH. The results are presented in Fig. 1. The graph shows that dye sorption lessened at high pH value. At pH 2 for Reactive Yellow-41 and Direct Blue-7 dyes, the removal capacity is high.

At low pH, there is a strong interaction between dye molecules and positively charged surface of the biomass [16]. Colak et al. [17] observed a similar kind of behavior for acid dye removal by *Paenibacillus macerans*.

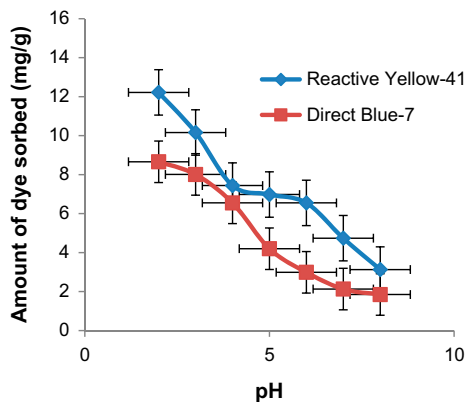


Fig. 1. Effect of pH on the biosorption of Reactive Yellow-41 and Direct Blue-7 dyes.

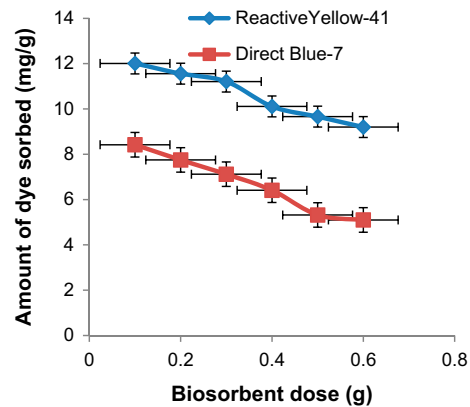


Fig. 2. Effect of biosorbent dose on the biosorption of Reactive Yellow-41 and Direct Blue-7 dyes.

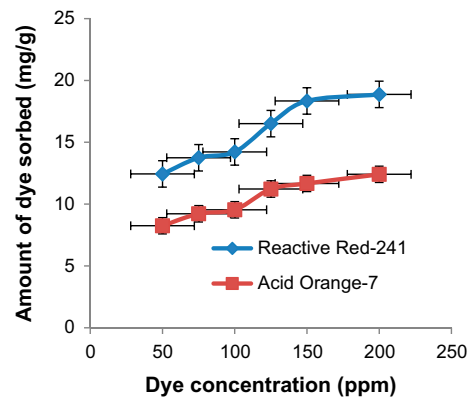


Fig. 3. Effect of dye concentration on the biosorption of Reactive Yellow-41 and Direct Blue-7 dyes.

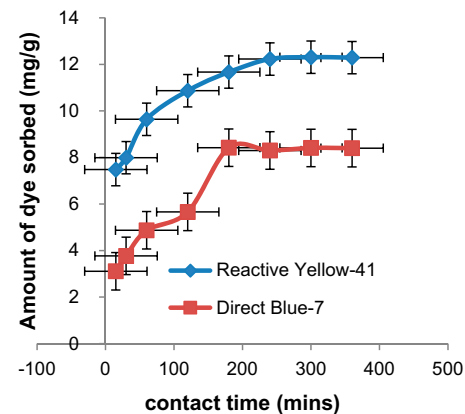


Fig. 4. Effect of contact time on the biosorption of Reactive Yellow-41 and Direct Blue-7 dyes.

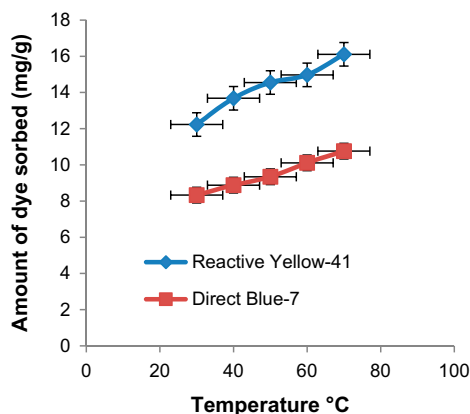


Fig. 5. Effect of temperature on the biosorption of Reactive Yellow-41 and Direct Blue-7 dyes.

3.2. Effect of the biocomposite dose

The influence of the biocomposite dose on the biosorption of Reactive Yellow-41 and Direct Blue-7 dyes on the wheat bran/zinc aluminum biocomposite and tea leaf waste/zinc aluminum biocomposite was measured by using different biocomposite doses and results are shown in Fig. 2. At high biocomposite dose, the biosorption capacity is minimum. The amount of dye removal increases from 18.00 to 22.44 mg/g for Reactive Yellow-41 dye onto wheat bran/zinc aluminum biocomposite and from 10.01 to

13.54 mg/g for Direct Blue-7 dye onto tea leaves waste/zinc aluminum biocomposites. Usually, the dye biosorption decreases with an increase in the biocomposite dosage, because binding sites of biocomposite decrease due to the accumulation of the biomass [18]. Ahmad et al. [19] showed that at high biomass dosage, the biosorption of direct dye declined. A similar trend was shown by the biosorption of anionic dyes onto rice husk waste [20].

3.3. Effect of the initial concentration of dye

Dye removal capacity is also influenced by the concentration of dye. There is a strong interaction between dye concentration and binding sites on a biocomposite surface. The effect of concentration of Reactive Yellow-41 and Direct Blue-7 dyes on the biosorption ability of biocomposites was investigated from 50 to 200 ppm concentration range. The data are presented in Fig. 3. The graph shows that the increase in dye biosorption is directly proportional to the dye concentration. The amount of Reactive Yellow-41 dye adsorbed increases from 17.54 to 26.89 mg/g onto the wheat bran/zinc aluminum biocomposite and from 10.01 to 16.99 mg/g for Direct Blue-7 dye onto the tea leaves waste/zinc aluminum biocomposite. Biosorption capacity of dye was enhanced because dye molecules biosorbed onto the outer surface and then penetrate inside the biomass [19].

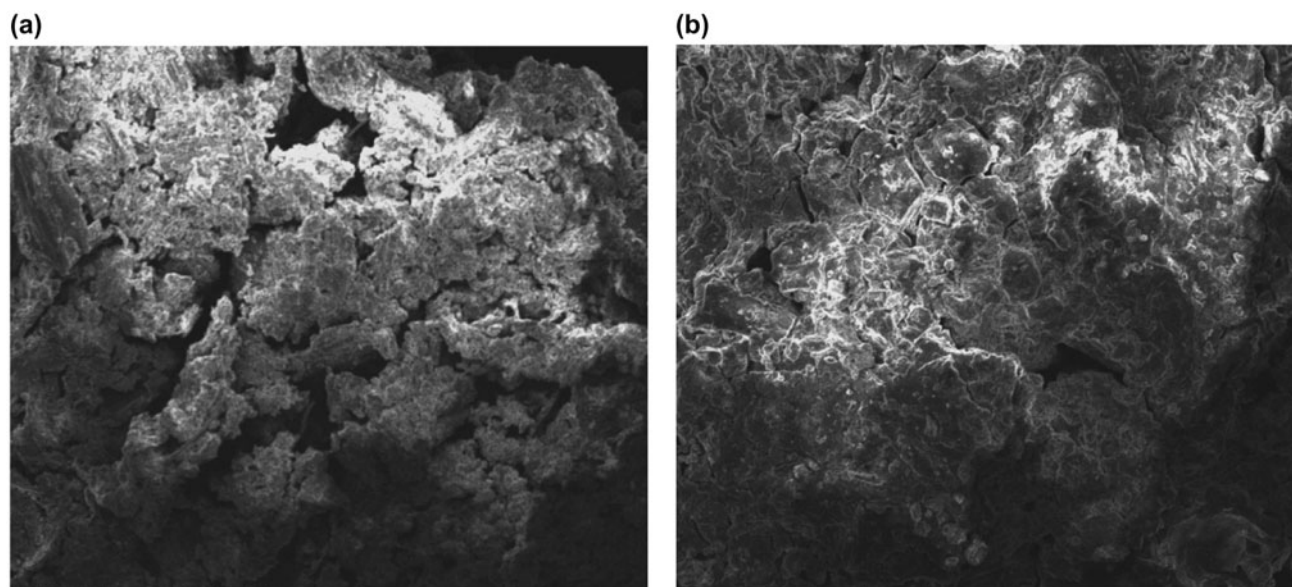


Fig. 6. SEM photographs of dye-loaded wheat bran/zinc aluminum biocomposite: (a) 500 micrometer and (b) 50 micrometer.

In 2009, Tunc et al. [21] described the removal of Remazol Black B dye from aqueous solutions and showed a similar behavior.

3.4. Effect of contact time

Biosorption capacity increases mostly with time rapidly. But further increase shows no remarkable change. It is shown in Fig. 4. The equilibrium biosorption time for Reactive Yellow-41 dye is 240 min and for Direct Blue-7 dye is 180 min after that there is no key increase in biosorption. Waranusantigul et al. [22] explained that the rate of biosorption of basic dye onto duckweed increased with the increase in the shaking time. Akar et al. [23] also showed the same trend for the biosorption of acid blue 40.

3.5. Effect of temperature

The effluents of industries have mostly a high temperature. Fig. 5 shows the effect of temperature of Reactive Yellow-41 and Direct Blue-7 dyes on biocomposites. The results describe that as temperature rises from 30 to 70°C, the removal capacity of biocomposite also increases. With increase in temperature the motion of dye molecules also increases. The increase in the amount of dye adsorption with the increasing temperature may be due to the increase in the energy of the large dye molecules [24]. Aksu and Tezer [25] showed the same behavior of reactive dye biosorption.

3.6. Biosorption kinetic models

In this research, pseudo-first-order and pseudo-second-order kinetic models are used to explain the biosorption kinetics.

3.6.1. Pseudo-first-order kinetic model

The principal of pseudo-first-order kinetic model is that the dye concentration changes with time. The differential equation is shown as follows:

$$dq_t/dt = k_1(q_e - q_t) \quad (4)$$

where q_e and q_t are biosorption capacities (mg/g) at equilibrium and time t , respectively, k_1 is the rate constant (1/min).

After interacting the above equation and applying boundary conditions $t = 0 - t = t$ and $q_t = 0 - q_t = q_t$, the equation becomes:

$$\log(q_e/q_e - q_t) = (k_1/2.303)t \quad (5)$$

After rearranging:

$$\log(q_e - q_t) = \log q_e - (k_1/2.303)t \quad (6)$$

The values of q_e (experimental), q_e (calculated), R^2 , and k_1 of both dyes are presented in Table 2.

The results describe that the calculated and experimental value of q_e does not relate and the value of R^2 is not acceptable in both dyes. So, the pseudo-first-order model is not well fitted.

3.6.2. Pseudo-second-order kinetic model

Pseudo-second-order kinetic model described the biosorption process over a wide range.

Pseudo-second-order kinetic equation is shown below:

$$dq_t/dt = k_2(q_e - q_t) \quad (7)$$

where k_2 (g/mg min) is the second-order rate constant for the biosorption process, q_e and q_t are the biosorption capacities at equilibrium and time t , respectively.

By integrating and applying boundary conditions $t = 0 - t = t$ and $q_t = 0 - q_t = q_t$, the above equation can be written in the linear form as follows:

$$t/q_t = 1/k_2q_e^2 + 1/q_e(t) \quad (8)$$

Table 2

Comparison of the kinetic parameters for the biosorption of Reactive Yellow-41 and Direct Blue-7 dyes onto wheat bran/zinc aluminum biocomposite and tea leaves waste/zinc aluminum biocomposite

Kinetic models	Reactive Yellow-41	Direct Blue-7
<i>Pseudo-first-order</i>		
k_1 (1/min)	0.0447	0.0011
q_e (experimental)	12.143	8.287
q_e (calculated)	3.007	1.121
R^2	0.533	0.457
<i>Pseudo-second-order</i>		
k_2 (g/mg min) 10^{-3}	0.2117	0.0629
q_e (experimental)	12.143	8.287
q_e (calculated)	2.214	2.001
R^2	0.994	0.982

The results are shown in Table 3. The values of q_e and R^2 for dyes are satisfactory and the model is well fitted to kinetic data.

Ozacar and Sengil [26] showed that the reactive dyes biosorption followed the second-order kinetic model. Ncibi et al. [27] observed that the biosorption of dye by *Posidonia oceanica* (L.) leaf sheaths obeyed the pseudo-second-order models.

3.7. Adsorption isotherms

The adsorption isotherm describes the interaction of adsorbate with adsorbent. In this work, two Langmuir isotherm and Freundlich isotherms are used.

3.7.1. Langmuir isotherm

The Langmuir isotherm is used for the biosorption of contaminants from aqueous solution. The surface phase may be considered as a monolayer or multilayer. Langmuir isotherm is based on the ideal monolayer adsorbed model. Langmuir isotherm is represented by the following equation:

$$C_e/q_e = 1/Kq_m + C_e/q_m \quad (9)$$

where C_e is the concentration of dye solution (mg/L) at equilibrium. The constant q_m signifies the adsorption capacity (mg/g) and K is related to the energy of adsorption (L/mg). Values of q_m and K are shown in Table 3.

3.7.2. Freundlich isotherm

The basic principal of this model is that the biosorption occurs by interacting the dye molecules on

the heterogeneous surfaces. The Freundlich isotherm form is given by the following equation:

$$q_e = K_F(C_e)^{1/n} \quad (10)$$

where q_e is the amount adsorbed per unit mass of the adsorbent (mg/g), C_e is the equilibrium concentration of the adsorbate (mg/L), and K_F , n are the Freundlich constants related to adsorption capacity and intensity, respectively. The logarithmic form of Eq. (10) gives the following linearized expression:

$$\ln q_e = \ln K_F + 1/n \ln C_e \quad (11)$$

The values of Freundlich constant n are given in Table 3 which shows that the model is best fitted. Ozacar and Sengil [26] studied that the removal of reactive dyes onto calcinated alunite obeyed the second-order kinetic model.

3.8. FT-IR studies

The FT-IR spectra of wheat bran/zinc aluminum biocomposite and tea leaves waste/zinc aluminum biocomposite before and after biosorption of Reactive Yellow-41 and Direct Blue-7 dyes were studied in the range of 400–4,000 cm^{-1} . The FT-IR spectra show the exchanging sites and functional groups on which biosorption takes place. The FT-IR spectra of biocomposites and peaks at 2,910.12 cm^{-1} of C–H stretching describe the presence of –CH and =CH groups which show that sugarcane bagasse and apple peel contain lignin and these outcomes are very similar to the described results. The band at 1,704.21 cm^{-1} can be assigned to C=O stretching vibrations. The peaks at 2,988.79 cm^{-1} represent the vibrations of –OH functional groups. The peaks appear due to C=O and –OH vibrations attribute the presence of carboxyl group on the surface of the biocomposite. The existence of peak at 1,633.33 cm^{-1} and bifurcated peak at 3,651.25 and 3,637.75 cm^{-1} may be due to the existence of amide group on the surface [28]. Due to definite interaction of biocomposite with dyes, alterations in the spectra are seen due to disappearing and broadening of some peaks. The –OH stretching peaks in dyes-loaded biocomposite vanish or absorb at lower frequency which shows the involvement of hydroxyl and carboxyl functional groups in the sorption mechanism. The intensity of –NH peak at 1,655.11 cm^{-1} decreased and the disappearance of bifurcation at higher frequency suggest that amide group also participates in the biosorption of dyes.

Table 3

Comparison of the isotherm parameters for the biosorption of Reactive Yellow-41 and Direct Blue-7 dyes onto wheat bran/zinc aluminum biocomposite and tea leaves waste/zinc aluminum biocomposite

Isotherm models	Reactive Yellow-41	Direct Blue-7
<i>Langmuir</i>		
R_L	0.411	0.278
R^2	0.995	0.989
q_m	24.012	9.411
<i>Freundlich</i>		
K_F	3.154	1.221
R^2	0.421	0.662
N	0.237	0.126

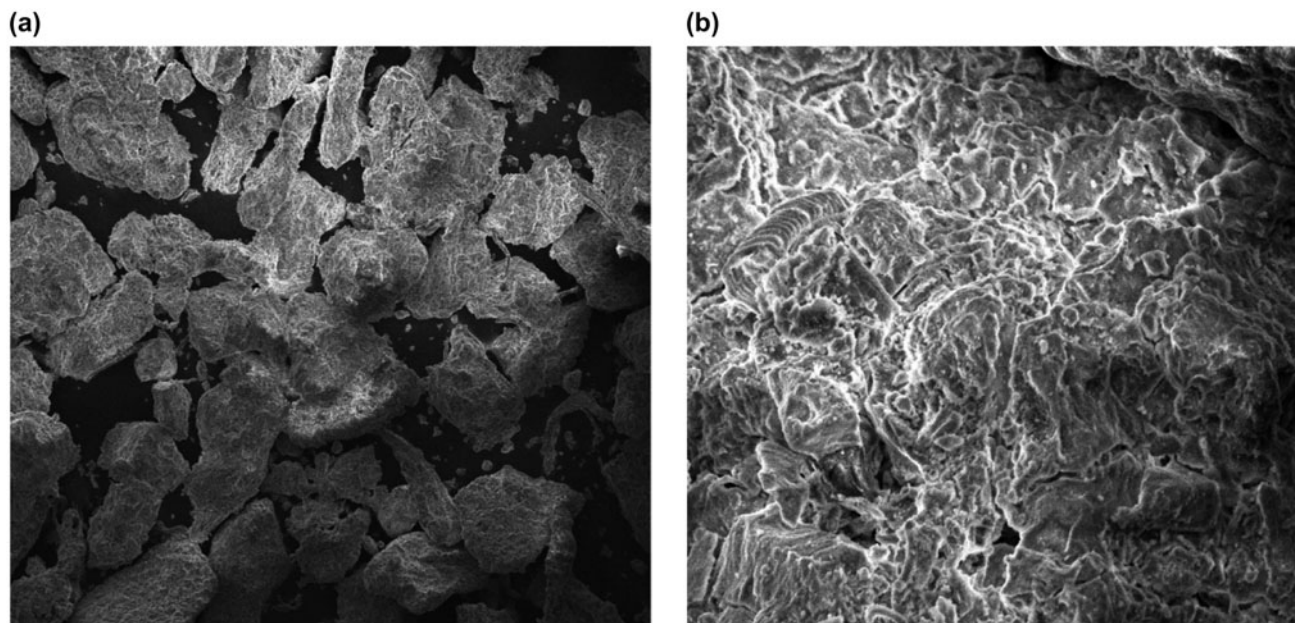


Fig. 7. SEM photographs of dye-loaded tea leaves waste/zinc aluminum biocomposite: (a) 500 micrometer and (b) 50 micrometer.

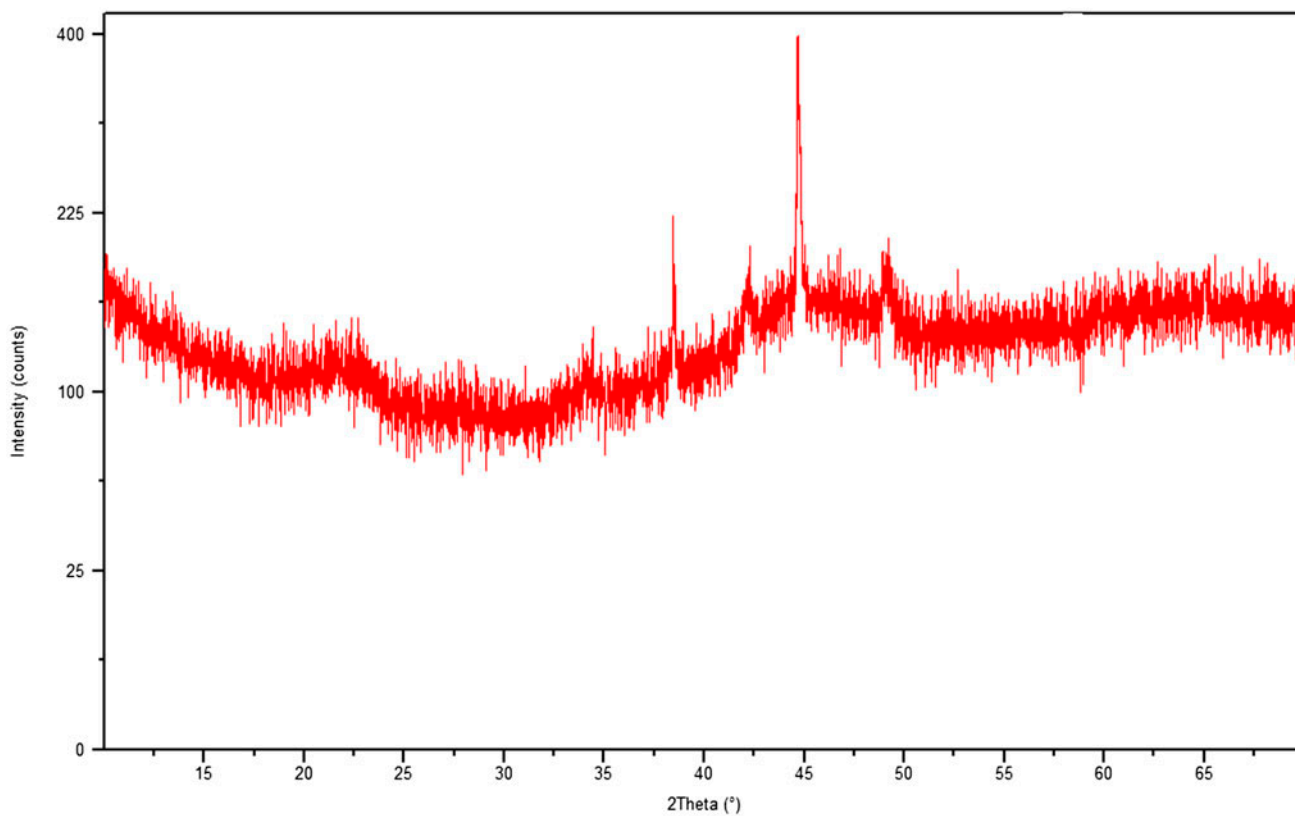


Fig. 8. XRD pattern of dye-loaded wheat bran/zinc aluminum biocomposite.

Table 4
Comparison of current study with data reported in literature

Biosorbent	Adsorption capacity (mg/g)	Refs.
Green algal spirogyra	6.2	[31]
Calcinated bones	81.67	[32]
Egg shells	28.87	[33]
Wheat bran biocomposite	17.87	Present study
Tea leaves biocomposite	10.01	Present study

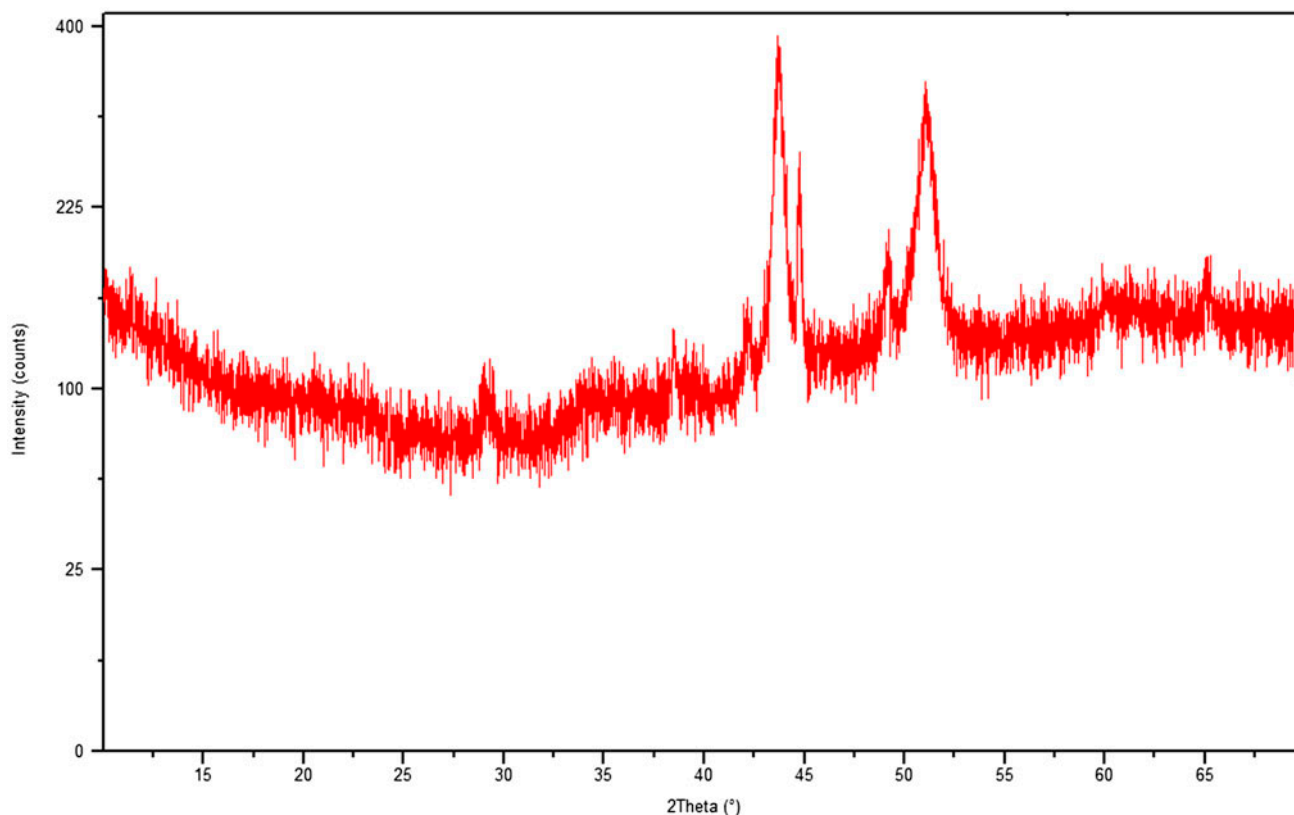


Fig. 9. XRD pattern of dye-loaded tea leaves waste/zinc aluminum biocomposite.

3.9. SEM analysis

SEM is used to illustrate the surface structure and morphology of the biosorbent material. It is used to define the shape and structure of biomass. Biosorption will be increased with more pores on the biomass surface [28]. Figs. 6(a, b) and 7(a, b) depict the morphology of dye-loaded wheat bran/zinc aluminum biocomposite and tea leaves waste/zinc aluminum biocomposite, respectively. On the surface of both the biocomposites, formation of white monolayer covering comes after biosorption of dyes. The confirmation of monolayer coverage was done by the Langmuir adsorption isotherm studies in batch condition. Akar

et al. [29] observed the surface morphology of untreated and dye-treated olive pomace biomass. The biocomposite surface exhibited the presence of dye molecules after sorption.

3.10. XRD analysis

X-ray diffraction is a proficient technique used to illustrate the crystallinity of compounds. Sharp and well-observed peaks were seen for crystalline compounds and diffused peaks were observed for amorphous substances. XRD pattern of dye-loaded biocomposites (wheat bran/zinc aluminum biocomposite

and tea leaves waste/zinc aluminum biocomposite) shows diffused peaks (Figs. 7 and 8). The XRD pattern of Reactive Yellow-41 and Direct Blue-7 dye after biosorption showed that the sharp peaks converted into diffused peaks and the crystalline nature of biomass changed into amorphous one. Namasivayam and Kavitha [30] described that *Carpinus betulus* showed well-observed peaks which converted into diffused form after biosorption of dyes. A comparative study of biosorption of some dyes is shown in Table 4.

3.11. Regeneration/reuse of the composite biomass

Regeneration of any adsorbent makes it economical as it can be used again many times without much cost. Nowadays the majority of adsorbents chosen are on the basis of effective regenerating capability. The type of adsorbate is very important in this respect like adsorbent and the process followed. The adsorption of all the dyes occurred at lower pH so now higher pH was required to desorb the dye. Distilled water with pH 10–14 was used for the desorption process.

A biocomposite surface attains negative charge when the pH of the solution is increased. And hence repulsion between negatively charged surface and anionic dye molecules causes their release back into solution form. The fact for using water was that it was costless, solubility, and easy to manage. The biocomposites were desorbed effectively up to five cycles with a little reduction in sorption capacity after each desorption cycle (Fig. 9).

4. Conclusions

The elimination of Reactive Yellow-41 and Direct Blue-7 dyes from aqueous solution by biosorption onto wheat bran/zinc aluminum biocomposite and tea leaves waste/zinc aluminum biocomposite was determined experimentally. The percentage removal of dyes was influenced by various process parameters. A high temperature enhances the biosorption rates. The equilibrium time was found to be 1 h (60 min) for Reactive Yellow-41 dye and 90 min for Direct Blue-7 dye. Maximum biosorption was observed at pH 2. The removal capacity of dyes decreases with more biomass because of a decrease in the biosorption sites. At elevated temperature, the biosorption capacity was enhanced because the motion of dye particles increases. Pseudo-second-order kinetic model and the Langmuir isotherm are well fitted to data. Characterization of the biocomposites was done through FT-IR, SEM, and XRD analysis.

References

- [1] H. Wang, Y. Huang, Prussian-blue-modified iron oxide magnetic nanoparticles as effective peroxidase-like catalysts to degrade methylene blue with H₂O₂, *J. Hazard. Mater.* 191 (2011) 163–169.
- [2] H. Hou, R. Zhou, P. Wu, L. Wu, Removal of Congo red dye from aqueous solution with hydroxyapatite/chitosan composite, *Chem. Eng. J.* 211–212 (2012) 336–342.
- [3] Y. Safa, Utilization of mustard and linseed oil cakes: Novel biosorbents for removal of acid dyes, *Desalin. Water Treat.* 57 (2016) 5914–5925.
- [4] Y. Safa, H.N. Bhatti, Biosorption of Direct Red-31 and Direct Orange-26 dyes by rice husk: Application of factorial design analysis, *Chem. Eng. Res. Des.* 89 (2011) 2566–2574.
- [5] T. Madrakian, A. Afkhami, M. Ahmadi, Adsorption and kinetic studies of seven different organic dyes onto magnetite nanoparticles loaded tea waste and removal of them from wastewater samples. *Spectrochim. Acta Part A Mol. Biomol. Spectrosc.* 99 (2012) 102–109.
- [6] N. Feng, X. Guo, S. Liang, Adsorption study of copper (II) by chemically modified orange peel, *J. Hazard. Mater.* 164 (2009) 1286–1292.
- [7] P.K. Malik, Use of activated carbons prepared from sawdust and rice-husk for adsorption of acid dyes: A case study of Acid Yellow 36, *Dyes Pigm.* 56 (2003) 239–249.
- [8] L.S. Chan, W.H. Cheung, G. McKay, Adsorption of acid dyes by bamboo derived activated carbon, *Desalination* 218 (2008) 304–312.
- [9] A. Khaled, A. El-Nemr, A. El-Sikaily, O.A. Wahab, Removal of Direct N Blue-106 from artificial textile dye effluent using activated carbon from orange peel: Adsorption isotherm and kinetic studies, *J. Hazard. Mater.* 165 (2009) 100–110.
- [10] P. Geetha, M.S. Latha, M. Koshy, Biosorption of malachite green dye from aqueous solution by calcium alginate nanoparticles: Equilibrium study, *J. Mol. Liq.* 212 (2015) 723–730.
- [11] T. Langmuir, The constitution and fundamental properties of solids and liquids, *J. Am. Chem. Soc.* 38 (2000) 2221–2295.
- [12] H.M.F. Freundlich, Over the adsorption in solution, *J. Phys. Chem.* 57 (1906) 385–407.
- [13] S. Lagergren, Zur Theorie der sogenannten Adsorption gelöster Stoffe (Theories of biosorption mechanisms), *Handlingar* 24 (1898) 1–39.
- [14] Y.S. Ho, G. McKay, D.A.J. Wase, C.F. Forster, Study of the sorption of divalent metal ions on to peat, *Adsorpt. Sci. Technol.* 18 (2000) 639–650.
- [15] Y. Safa, Biosorption of Eriochrome Black T and Astrazon FGGL Blue using almond and cotton seed oil cake biomass in a batch mode, *J. Chem. Soc. Pak.* 36 (2014) 614–623.
- [16] A. Nemr, O. Abdelwahab, A. El-Sikaily, A. Khaled, Removal of direct blue-86 from aqueous solution by new activated carbon developed from orange peel, *J. Hazard. Mater.* 161 (2009) 102–110.
- [17] F. Çolak, N. Atar, A. Olgun, Biosorption of acidic dyes from aqueous solution by *Paenibacillus macerans*: Kinetic, thermodynamic and equilibrium studies, *Chem. Eng. J.* 150 (2009) 122–130.

- [18] J. Tangaromsuk, P. Pokethitiyook, M. Kruatrachue, E.S. Upatham, Cadmium biosorption by *Sphingomonas paucimobilis* biomass, *Bioresour. Technol.* 85 (2002) 103–105.
- [19] A.A. Ahmad, B.H. Hameed, N. Aziz, Adsorption of direct dye on palm ash: Kinetic and equilibrium modeling, *J. Hazard. Mater.* 141 (2007) 70–76.
- [20] H.N. Bhatti, Y. Safa, Removal of anionic dyes by rice milling waste from synthetic effluents: Equilibrium and thermodynamic studies, *Desalin. Water Treat.* 48 (2012) 267–277.
- [21] Ö. Tunç, H. Tanacı, Z. Aksu, Potential use of cotton plant wastes for the removal of Remazol Black B reactive dye, *J. Hazard. Mater.* 163 (2009) 187–198.
- [22] P. Waranusantigul, P. Pokethitiyook, M. Kruatrachue, E.S. Upatham, Kinetics of basic dye (methylene blue) biosorption by giant duckweed (*Spirodela polyrrhiza*), *Environ. Pollut.* 125 (2003) 385–392.
- [23] T. Akar, A.S. Ozcan, S. Tunali, A. Ozcan, Biosorption of a textile dye (Acid Blue 40) by cone biomass of *Thuja orientalis*: Estimation of equilibrium, thermodynamic and kinetic parameters, *Bioresour. Technol.* 99 (2008) 3057–3065.
- [24] Y.P. Wei, H.W. Gao, SN @ silicate: An anionic dye sorbent and its reuse, *J. Mater. Chem.* 22 (2012) 5715–5722.
- [25] Z. Aksu, S. Tezer, Biosorption of reactive dyes on the green alga *Chlorella vulgaris*, *Process Biochem.* 40 (2005) 1347–1361.
- [26] M. Ozacar, I.A. Sengil, Adsorption of reactive dyes on calcinated alunite from aqueous solutions, *J. Hazard. Mater.* 40 (2003) 1–14.
- [27] M.C. Ncibi, B. Mahjoub, A.M. Hamissa, R. Ben Mansour, M. Seffen, Biosorption of textile metal-complexed dye from aqueous medium using *Posidonia oceanica* (L.) leaf sheaths: Mathematical modelling, *Desalination* 243 (2009) 109–121.
- [28] Y. Safa, H.N. Bhatti, Adsorptive removal of direct textile dyes by low cost agricultural waste: Application of factorial design analysis, *Chem. Eng. J.* 167 (2011) 35–41.
- [29] T. Akar, B. Anilan, A. Gorgulu, S.T. Akar, Assessment of cationic dye biosorption characteristics of untreated and non-conventional biomass: *Pyraecantha coccinea* berries, *J. Hazard. Mater.* 168 (2009) 1302–1309.
- [30] C. Namasivayam, D. Kavitha, IR, XRD and SEM studies on the mechanism of adsorption of dyes and phenols by coir pith carbon from aqueous phase, *Microchem. J.* 82 (2006) 43–48.
- [31] A.R. Khataee, F. Vafaei, M. Jannatkah, Biosorption of three textile dyes from contaminated water by filamentous green algal *Spirogyra* sp.: Kinetic, isotherm and thermodynamic studies, *Int. Biodeterior. Biodegrad.* 83 (2013) 33–40.
- [32] M. Ei Haddad, R. Slimani, R. Mamouni, M.R. Laamari, S. Rafqah, S. Lazar, Evaluation of potential capability of calcinated bones on the biosorption removal efficiency of Saranin as cationic dye from aqueous solution, *J. Taiwan Inst. Chem. Eng.* 44 (2013) 13–18.
- [33] R. Slimani, I.E.I. Quahabi, F. Abidi, M.E.I. Haddad, A. Regti, M.R. Laamari, S.E.I. Antri, S. Lazar, Calcined eggshells as a new biosorbent to remove basic dye from aqueous solutions: Thermodynamics, kinetics, isotherms and error analysis, *J. Taiwan Inst. Chem. Eng.* 45 (2014) 1578–1587.